ISSN 2517-7516, Membranes and Membrane Technologies, 2020, Vol. 2, No. 5, pp. 283–295. © Pleiades Publishing, Ltd., 2020.
Russian Text © The Author(s), 2020, published in Membrany i Membrannye Tekhnologii, 2020, Vol. 2, No. 5, pp. 295–308.

Structure and Properties of Polyethersulfone Membranes Based on Polyethersulfone–Nonsolvent–Solvent Systems

A. V. Bildyukevich[a], T. A. Hliavitskaya[a, *], and G. B. Melnikova[b]

[a] *Institute of Physical Organic Chemistry, National Academy of Sciences of Belarus, Minsk, 220072 Republic of Belarus*
[b] *Lykov Heat and Mass Transfer Institute, National Academy of Sciences of Belarus, Minsk, 220072 Republic of Belarus*
**e-mail: hlyavitskaya1706@gmail.com*

Received May 10, 2020; revised May 24, 2020; accepted June 11, 2020

Abstract—The effect of degree of saturation of casting solutions (α*—the ratio of the nonsolvent amount added to the polymer solution to the non-solvent amount which causes phase separation) and nonsolvent power on the structure and performance of membranes prepared from system "Polyethersulfone (PES)–non-solvent–solvent" have been studied. Nonsolvent power has been characterized in terms of precipitation number (PN), i.e., the amount of nonsolvent that leads to phase separation of 100 mL of a 1% PES solution. Glycerol (PN = 27.8 g/dL), polyethylene glycol 400 (PN > 1000 g/dL), and their mixtures have been used as a nonsolvent additive to the casting solution. It has been shown that membranes with a nice spongy structure are formed in the case of using casting solutions located near the binodal line. In this case, the membrane flux depends on the nonsolvent power: the higher the PN of the nonsolvent, the higher the membrane flux. The highest flux is exhibited by membranes prepared from casting solutions with a degree of saturation of α* = 0.52–0.81 depending on the PN of the nonsolvent. In this case, macrovoids are present in the structure of the supporting layer of the membranes; the size and shape of the macrovoids also depend on the PN of the nonsolvent: the higher the PN, the larger the macrovoid size in the membrane supporting layer. The results have made it possible to propose a new approach to obtaining PES membranes with a desired structure and properties.

Keywords: phase inversion, polyethersulfone, nonsolvent, precipitation number, degree of saturation
DOI: 10.1134/S2517751620050029

INTRODUCTION

Polyethersulfone (PES) has found wide application as a membrane-forming material owing to an exceptional set of characteristics, namely, a high chemical and thermal stability, mechanical strength, and the relative ease of membrane preparation in various configurations. The main PES membrane preparation method is phase inversion in various versions: immersion precipitation (nonsolvent-induced phase separation), thermal precipitation (thermally induced phase separation), precipitation by evaporation (evaporation-induced phase separation), and precipitation in vapour phase (vapor-induced phase separation) [1–3]. Membrane formation by immersion precipitation (nonsolvent-induced phase separation) occurs owing to mass transfer between the solvent from the casting solution and the nonsolvent (coagulant) in a coagulation bath (typically water) [4]. The main requirement for the initial casting solution is homogeneity; that is, in the polymer–nonsolvent–solvent ternary phase diagram, the solution composition should lie in the miscibility gap region [1–5]. Membranes prepared by immersion precipitation are most commonly characterized by the presence of a large number of macrovoids in the substructure of the supporting layer. It is known that the size and structure of these macrovoids can have a significant effect on the flux and mechanical strength of the membranes. The presence of macrovoids in the membrane substructure is undesirable because it is believed that their presence can lead to a deterioration of the selective layer upon the application of a working pressure [6, 7]. The introduction of a nonsolvent into the casting solution composition is one of the key methods to control the membrane structure (elimination of macrovoids) and flux. Typically, membranes prepared from these solutions have a pronounced spongy structure; that is, they are characterized by the absence of macrovoids in the supporting layer [6, 8–11]. A wide range of compounds: water, monohydric and polyhydric alcohols, glycols, organic acids, etc., and mixtures of various nonsolvents can be used as a nonsolvent additive to casting solutions [12–21].

The introduction of a nonsolvent into the casting solution has a significant effect on the stability and the viscous properties of the casting solutions, which in turn affects the membrane flux [6, 14, 22–25].

The introduction of a nonsolvent into the casting solution brings the composition closer to the binodal line in the polymer–nonsolvent–solvent ternary phase diagram; it is one of the key methods for both controlling the membrane structure and permeability and eliminating macrovoids [9, 26]. Several approaches are used to determine the position of the casting solution composition relative to the binodal line in the polymer–nonsolvent–solvent ternary phase diagram. Some authors use the "approaching ratio" (α) for this purpose; it is defined as the nonsolvent-to-solvent weight ratio in the casting solution to the nonsolvent-to-solvent weight ratio at the cloud point [27–30]. The authors of [6] introduced the concept of "degree of saturation" of the casting solution (α^*), which is understood as the ratio of the amount of the nonsolvent introduced into the system to the limiting amount that leads to the separation of the system into two phases. Below, it will be shown that the two approaches give comparable results.

Wang proposed that the casting solution composition should be characterized using the "precipitation ratio" ($R_{a/s}$) [31–33]. This ratio is defined as the nonsolvent-to-solvent weight ratio in the casting solution, although the use of this parameter is highly disputable, because this parameter does not provide any information about the position of the solution in the ternary phase diagram.

It should be noted that different nonsolvents exhibit different affinities for the polymer; this factor affects the miscibility region area in the ternary phase diagram (binodal position) and the viscosity of polymer solutions [6, 22–24, 30].

To characterize a nonsolvent in a casting solution and determine the effect of the coagulation bath composition on the structure and properties of the membranes, the precipitation value (PV) or coagulation value (CV) quantities are used [25, 31–41]. In the production of chemical fibers, to characterize the precipitation ability (power) of a particular nonsolvent with respect to a given polymer–solvent system; in particular, to determine the power of a coagulation bath, precipitation number (PN) is used. The PN is defined as the amount of nonsolvent that leads to the phase separation of 100 mL of a 1% polymer solution and expressed in terms of g/dL [34, 41, 42]. Wang et al., [31–33] used PV (amount of nonsolvent required for clouding a polymer solution containing 2 g of a polymer and 100 g of a solvent) to select the casting solution composition and an appropriate nonsolvent to the coagulation bath.

In the literature, there are significant methodological differences in determining the CV parameter; they are associated with the titrated solution volume and concentration and, accordingly, with the units of CV. Lai et al. [37], determined CV by ethanol titration of a polymer solution containing 1 g of poly(4-ethyl-1-pentene), 23.75 mL of cyclohexane, and 3.75 mL of various nonsolvents. Titration was run at 40°C. It was found that the membrane porosity decreased with an increase in the CV [37]. Feng et al. [24], used CV to characterize the thermodynamic stability of 26% sulfonated polyphenylenesulfone casting solutions with the addition of PEG-400. In this case, CV is defined as the amount of water (nonsolvent) in grams that causes the phase separation of 10 g of the casting solution. A decrease in the CV owing to the addition of PEG-400 to the casting solution leads to the suppression of the formation of macrovoids in the membrane substructure, which is attributed to the accelerated kinetics of the phase separation process [24]. The effect of the use of acetone, ethanol, or water in a coagulation bath on the structure and properties of membranes based on the ethylene–vinyl alcohol copolymer was studied by Chen et al. [38]. The cited authors compared the CVs of various nonsolvents. Nonsolvents were added to a 15 wt % ethylene–vinyl alcohol copolymer solution at 25°C until cloudy. Chun et al. [40], tested various mixtures of dimethylacetamide (DMAA) and water as nonsolvents for the titration of 6.5 mL of 2 wt % polyimide solutions. The amount of the introduced nonsolvent was recorded as the CV value. It was found that an increase in the CV of the nonsolvent in the coagulation bath leads to a decrease in the specific pore volume on the membrane surface. It can be concluded that CV is an analog of PV. In general, PV or CV describes the phase separation process in the region of low concentrations of polymer solutions (<2%) and does not provide any information on the behavior of concentrated polymer solutions used for membrane preparation. Wang et al. [32], tried to determine a relationship between CV and precipitation ratio ($R_{a/s}$) for PES–*N*-methylpyrrolidone (NMP)–methanol, polysulfone–DMAA–methanol, PES–NMP–H_2O, polysulfone–DMAA–H_2O, and other systems. An equation for predicting the casting solution composition depending on the CV of nonsolvents was proposed; a satisfactory agreement between the calculated and experimental data was shown. However, all studies were conducted using the example of 2% polymer solutions.

A search of the literature has not revealed a clear relationship between the power of the nonsolvent (PN, PV, or CV parameters) in the casting solution and the membrane properties and structure. This failure is attributed to differences in methodological approaches and the fact that the position of the casting solution composition in the phase diagram relative to the binodal, i.e., the degree of saturation of the casting solution, is not taken into account. To eliminate the effect of the degree of saturation of the casting solution on the membrane structure and properties, in this study, solutions with $\alpha^* = 0.94–0.95$ are used.

The aim of this study is to determine a relationship between the nonsolvent power and the structure and properties of ultrafiltration membranes.

EXPERIMENTAL

Membranes were prepared using PES Ultrason E 6020P (M_w = 58000 g/mol, BASF, Germany). Glycerol (State Standard GOST 6259-75) and polyethylene glycol $\langle M_n \rangle$ = 400 g/mol (PEG-400, BASF, Germany) were used as a nonsolvent additive to the casting solution. The solvent was DMAA (BASF, Germany). Distilled water was used as the coagulant.

Casting solutions of PES in DMAA with glycerol and PEG-400 additives (as a nonsolvent) were prepared on a specially designed laboratory bench, which included a round-bottom glass flask and stirrer (IKARW 20 Digital, Germany). The solutions were prepared at a temperature of 90°C, a preparation time of 3 h, and a stirring rate of 400 rpm. In all the cases, the polymer concentration in the casting solution composition was constant—22%. The amount of nonsolvent (PEG-400–glycerol mixture) as an additive into the casting solution was calculated by multiplying an appropriate amount of the nonsolvent that causes phase separation of a 22% PES solution by the degree of saturation (α*). The degree of saturation of the casting solutions varied in a range of 0–0.95. Approaching ratio α was determined as the nonsolvent-to-solvent weight ratio in the casting solution to the nonsolvent-to-solvent weight ratio at the cloud point.

Membranes were prepared by immersion precipitation. The casting solution was deposited onto a glass plate using a casting knife with a slit width of 200 μm. The temperature of the coagulation bath was 23°C. The prepared membrane was washed from the residual solvent for 24 h and then impregnated with a 30% aqueous solution of glycerol to prevent pore contraction.

The PN was determined by titration of 100 mL of a 1% PES solution in DMAA (under constant stirring) with individual nonsolvents and their mixtures with PEG-400 in various weight ratios until visible turbidity; PN was expressed in terms of g/dL.

Pure water flux of the membranes (J_0, L/(m^2 h)) was calculated by formula

$$J_0 = V/(St), \quad (1)$$

where V is the permeate volume, L; S is the membrane working surface area, m^2; and t is the filtration time, h.

The rejection coefficient was calculated by formula

$$R = \left(1 - \frac{C_{perm}}{C_{feed}}\right) \times 100\%, \quad (2)$$

where C_{perm} is the calibrant concentration in the permeate (g/L) and C_{feed} is the calibrant concentration in the feed solution (g/L). The calibrant was a 0.3% aqueous solution of polyvinylpyrrolidone (PVP) K-30 (Fluka, Germany).

Membrane morphology was studied using a Phenom Pro scanning electron microscope (Thermo Fisher Scientific); samples for analysis were preconditioned by cryogenic fracturing in liquid nitrogen; after that, a layer of gold was deposited by cathodic sputtering on an EMITECH K 550X vacuum system (Germany).

The structure of the membrane selective layer was studied by atomic force microscopy (NT-206, Mikrotestmashiny, Belarus) using standard NSC35 silicon cantilevers (MikroMasch, Estonia) with a probe curvature radius of no more than 10 nm and a hardness of 3.5 N/m (according to the manufacturer's certificate).

RESULTS AND DISCUSSION

Choice of Nonsolvent

The following materials were used as potential nonsolvents with different precipitation numbers for introducing into a PES solution in DMAA: PEG-400 (PN > 1000 g/dL) as a weak nonsolvent; water (PN = 10.6 g/dL), 85% phosphoric acid (PN = 13.0 g/dL), and glycerol (PN = 27.8 g/dL) as stronger nonsolvents; and a mixture of weak and strong nonsolvents in various weight ratios. Results of determination of PN for PEG-400–water, PEG-400–phosphoric acid, and PEG-400–glycerol mixtures are shown in Fig. 1. It is evident that the PNs of the studied mixtures with respect to a 1% PES solution in DMAA vary in a wide range of 15–1000 g/dL. The dependence of PN on the concentration of components in the mixture is nonadditive. The effect of a stronger nonsolvent is dominant up to a PEG-400 concentration of 80%; after that, an abrupt increase in PN values is observed; it indicates a decrease in the nonsolvent power of the mixture. For glycerol–PEG-400 mixtures, the dependence of PN on the glycerol concentration is more gently sloping than that of water–PEG-400 and H_3PO_4–PEG-400 mixtures. The results suggest that the precipitation value (nonsolvent power) of the glycerol–PEG-400 mixture can be controlled over a wider range and confirm the prospects of using this mixture to study the effect of the power (PN) of a nonsolvent introduced into the casting solution composition on the membrane structure and properties.

According to the results, glycerol–PEG-400 mixtures selected for further studies (for introducing into the casting solution) had the following weight ratios of components: 100/0 (PN = 27.8 g/dL), 85/15 (PN = 39.7 g/dL), 70/30 (PN = 50.4 g/dL), 50/50 (PN = 78.3 g/dL), 40/60 (PN = 125 g/dL), 30/70 (PN = 250 g/dL), and 20/80 (PN = 750 g/dL).

Effect of the PN of the Nonsolvent on the Properties of the Casting Solution

Figure 2 shows (a) a ternary phase diagram of the PES–glycerol+PEG-400–DMAA system for glycerol–PEG-400 nonsolvents with different PN values and (b) a fragment of the phase diagram of the same

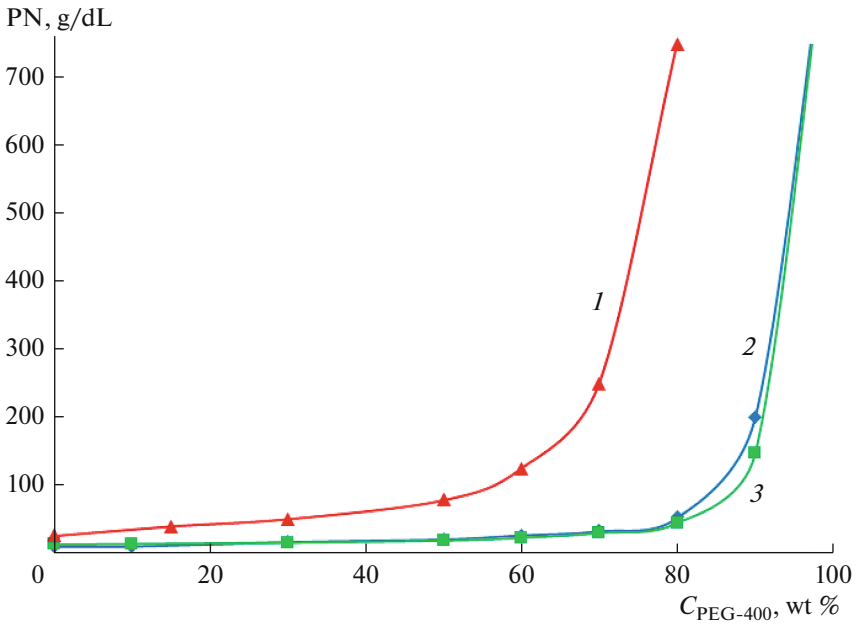

Fig. 1. Dependence of the PN of (*1*) glycerol–PEG-400, (*2*) water–PEG-400, and (*3*) H_3PO_4–PEG-400 mixtures on the PEG-400 concentration in the mixture.

system for a 22% PES solution. According to Fig. 2, an increase in the PN of the nonsolvent leads to an increase in the glycerol–PEG-400 concentration providing the formation of stable homogeneous solutions (binodal line is shifted toward the PES–nonsolvent axis, Fig. 2a); that is, the component miscibility gap is expanded. Thus, for a 22% PES solution, for a glycerol–PEG-400 mixture with PN = 39.7 g/dL, the maximum additive concentration was 18.7%; in the case of mixtures with PN = 125 and 750 g/dL, it was 32 and 42.5%, respectively. In the case of using individual PEG-400, the solution remained homogeneous even upon the introduction of 60% of the additive.

Results of viscometric studies of PES solutions with additives of glycerol–PEG-400 mixtures with different PN values are shown in Fig. 3. Regardless of the PN of the nonsolvent, the viscosity of the casting solution increases exponentially with an increase in the nonsolvent concentration. In general, the results are in good agreement with the available published data [44]. At a fixed additive concentration, a decrease in the PN of the nonsolvent leads to an increase in the dynamic viscosity of the PES solutions. Thus, upon the introduction of 15% of a nonsolvent into the casting solution composition, a gradual increase in the viscosity of the solutions with an increase in nonsolvent power is observed: for a nonsolvent with PN = 750 g/dL, the viscosity is 3.78 Pa s; for PN = 78.3 g/dL, 5.15 Pa s; and for PN = 50.4 g/dL, 6.05 Pa s. In the case of using weak nonsolvents (PN > 80 g/dL), the maximum additive concentration at which the casting solution was stable is significantly higher; therefore, the viscosity of casting solutions can be controlled over a wide range. Thus, upon the introduction of 15% of a glycerol–PEG-400 mixture with PN = 750 g/dL into the system, the viscosity is 3.78 Pa s, whereas at a nonsolvent content of 40%, the viscosity achieves 27.5 Pa s.

Effect of the Degree of Saturation of the Casting Solution and the PN of the Nonsolvent on the Membrane Structure and Properties

Membranes were prepared from PES–glycerol–PEG-400–DMAA four-component solutions using glycerol–PEG-400 mixtures with various PNs (39.7–750 g/dL) at a constant PES concentration (22%). This PES concentration was selected intentionally, because the membrane prepared from a 22% PES solution in DMAA is impermeable to water. The degree of saturation of the casting solutions (α^*) was varied in a range of 0–0.95.

The dependence of the membrane flux on the degree of saturation of casting solutions for different PN values of the nonsolvent is shown in Fig. 4. The membrane prepared from a 22% PES solution in DMAA ($\alpha^* = 0$) is impermeable to water ($J_0 = 0$ L/(m^2 h)) at a pressure of 1 atm. The subsequent increase in the degree of saturation to $\alpha^* = 0.59$–0.81 leads to a gradual increase in the membrane flux. Near the binodal line ($\alpha^* = 0.94$–0.95), the membrane flux decreases again; that is, the dependence of the membrane flux on the degree of saturation of the casting solution passes through a maximum. These results are in good agreement with data described earlier in [36, 45]. Thus, for nonsolvents with PN < 78.3 g/dL, the dependence exhibits a pronounced extreme character.

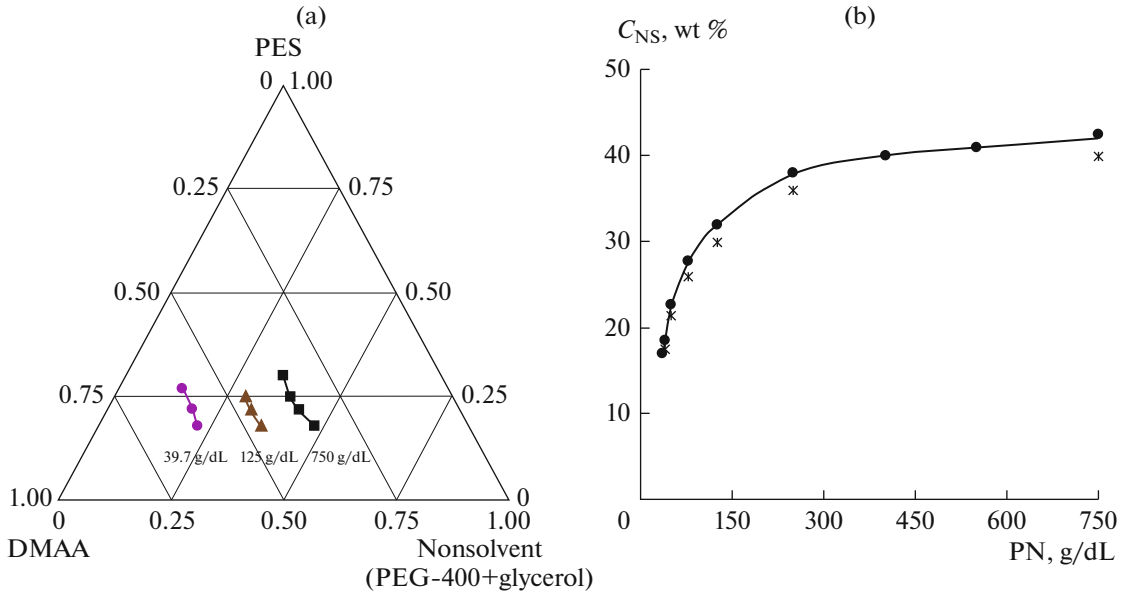

Fig. 2. (a) Phase diagram of a PES–glycerol+PEG-400–DMAA three-component system and (b) dependence of the maximum glycerol–PEG-400 nonsolvent (NS) mixture concentration in 22% PES solutions on the PN of the glycerol–PEG-400 mixture. The star-shaped marker indicates the compositions used to prepare the membranes.

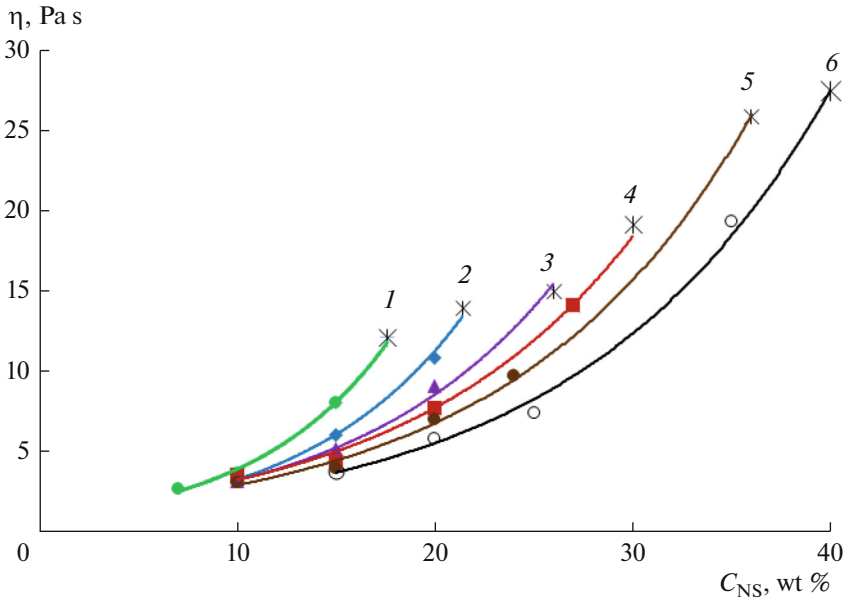

Fig. 3. Dependence of the viscosity of 22% PES–glycerol+PEG-400–DMAA solutions on the glycerol–PEG-400 nonsolvent concentration for different PNs: (*1*) 39.7, (*2*) 50.4, (*3*) 78.3, (*4*) 125, (*5*) 250, and (*6*) 750 g/dL. The star-shaped marker indicates the glycerol–PEG-400 nonsolvent concentrations corresponding to a degree of saturation of $\alpha^* = 0.94–0.95$ (at 25°C).

In the case of weak nonsolvents (PN > 78.4 g/dL), the dependence of the flux on the degree of saturation also passes through a maximum; however, in general, it is not so extreme. It was found that the highest water flux is exhibited by membranes prepared from casting solutions with a saturation degree of $\alpha^* = 0.59–0.81$ (depending on the PN of the nonsolvent). An increase in the membrane flux in this region can be attributed to the formation of supramolecular aggregates of a "critical" size in polymer solutions. This aggregates provide such high flux of ultrafiltration membranes [34, 36, 46].

Analysis of the transport properties of the membranes showed that the degree of saturation of casting

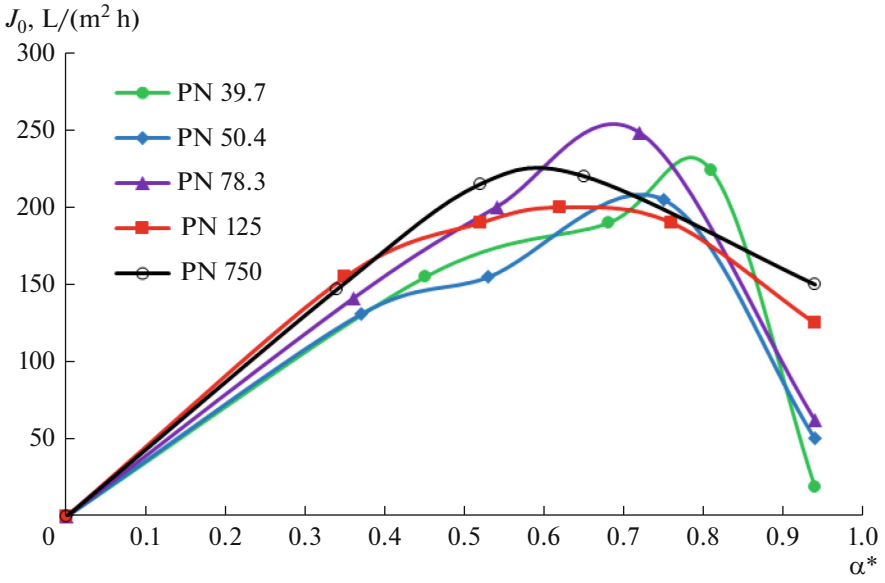

Fig. 4. Dependence of the membrane flux on the degree of saturation of the casting solution for different PN values of the nonsolvent in a range of 39.7–750 g/dL.

solutions corresponding to the maximum water flux of membranes ($\alpha^*(J_{max})$) varies in an extremely limited range. Figure 5 shows the dependence of $\alpha^*(J_{max})$ on the PN of the nonsolvent. It was found that an increase in the PN of the nonsolvent leads to a decrease in the degree of saturation of the casting solution corresponding to the maximum water flux of membranes. Thus, with an increase in the PN of the nonsolvent from 39.7 to 750 g/dL, $\alpha^*(J_{max})$ decreases from 0.81 to 0.59.

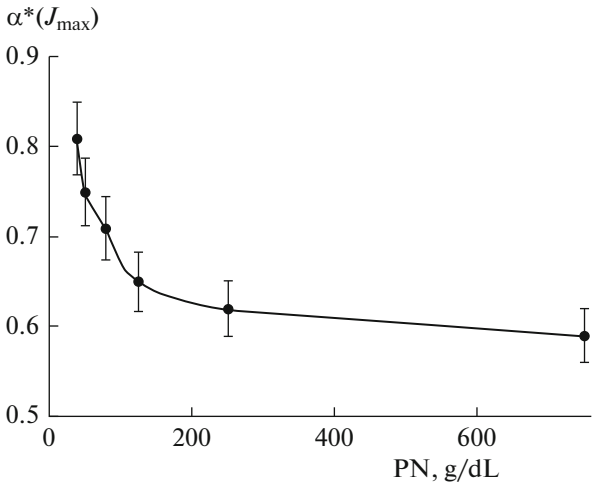

Fig. 5. Dependence of the degree of saturation corresponding to the maximum membrane flux on the PN of the nonsolvent.

Figure 6 shows the membrane structures as a function of the degree of saturation of the casting solution for a rather strong nonsolvent (PN = 78.3 g/dL) and for a weak nonsolvent (PN = 750 g/dL). At $\alpha^* = 0$, the structure of the membrane supporting layer contains a large number of macrovoids, which significantly vary in shape and size. An increase in the degree of saturation of the casting solution to $\alpha^* = 0.35–0.36$ contributes to the formation of a transition layer (between the selective and supporting layers) with a spongy structure (see Figs. 6b, 6c). At this degree of saturation ($\alpha^* = 0.35–0.36$), the use of nonsolvents with different PN values also affects the membrane structure. In the case of using a weak nonsolvent with PN = 750 g/dL, large-sized macrovoids were localized along the entire length of the membrane supporting layer; at PN = 78.3 g/dL, the macrovoids were significantly smaller. A similar relationship was observed for membranes prepared from casting solutions with a degree of saturation of $\alpha^* = 0.71–0.72$ (Figs. 6d, 6e). A further increase in the degree of saturation of casting solutions to $\alpha^* = 0.94$ led to the complete disappearance of macrovoids and the formation of completely spongy structures (Figs. 6f, 6g). Thus, it can be concluded that the initial PES–glycerol+PEG-400–DMAA casting solution contains elements of the future structure of polymer membranes, namely, a two-phase microheterogeneous system, which, upon subsequent coagulation, is transformed into a system of interpenetrating pores. In addition, the structure of the microheterogeneous system of the solution depends on both the degree of saturation of the casting solution and the PN of the introduced nonsolvent.

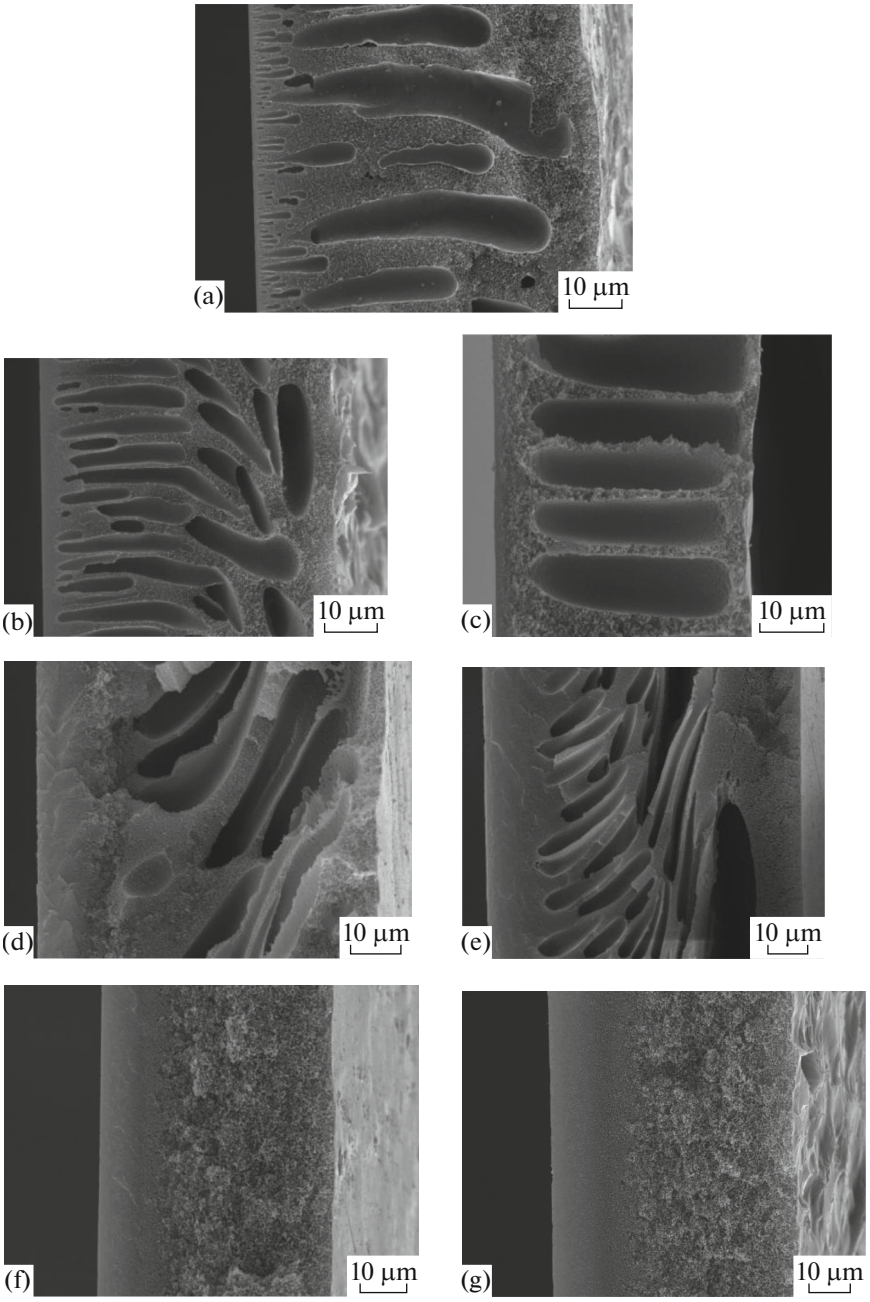

Fig. 6. Electron micrographs of the cross section structure of membranes prepared from PES–glycerol+PEG-400–DMAA solutions for the different degrees of saturation (α*) and PNs of the nonsolvent: (a) α* = 0; (b) α* = 0.36, PN = 78.3 g/dL; (c) α* = 0.35, PN = 750 g/dL; (d) α* = 0.72, PN = 78.3 g/dL; (e) α* = 0.71, PN = 750 g/dL; (f) α* = 0.94, PN = 78.3 g/dL; and (g) α* = 0.94, PN = 750 g/dL.

The next stage of the study was a detailed analysis of the effect of the PN of the nonsolvent on the structure and properties of membranes prepared from compositions lying near the binodal in the phase diagram, i.e., at α* = 0.94–0.95. This degree of saturation was selected intentionally to eliminate the presence of macrovoids in the supporting layer of the membranes [8]. Since both the amount of the introduced nonsolvent and the position of the resulting composition relative to the binodal (see Fig. 2) highly depend on the glycerol–PEG-400 mixture composition (i.e., the PN of the nonsolvent), to obtain comparable results (determine the effect of the PN of the nonsolvent on the membrane structure and properties and eliminate the mutual effect of the degree of saturation and PN), the composition of the casting solutions was selected so that they had similar degrees of saturation of α* = 0.94–0.95; that is, they should located near the

Table 1. Compositions and viscosity of casting solutions

Casting solution composition, wt %				PN of nonsolvent, g/dL	Degree of saturation α*	Approaching ratio (α)	Viscosity, Pa s
PES	glycerol	PEG-400	DMAA				
22	15.0	2.6	60.4	39.7	0.95	0.93	12.1
22	14.8	6.6	56.6	50.4	0.94	0.92	14.0
22	13.0	13.0	52.0	78.3	0.94	0.91	14.9
22	12.0	18.0	48.0	125	0.94	0.90	19.2
22	10.8	25.2	42.0	250	0.95	0.89	25.9
22	8.0	32.0	38.0	750	0.94	0.88	27.5

binodal. The respective compositions and their viscosity are listed in Table 1. Comparison of the degrees of saturation (α*) and the approaching ratios (α) showed that these characteristics of casting solutions have comparable values. Thus, the α value is lower than the degree of saturation of the casting solution by as little as 2–5%.

Figure 7 shows the effect of the PN of the nonsolvent on the pure water flux of the membranes (J_0) and PVP (K-30) rejection coefficient (R).

It is evident that, with an increase in the PN of the nonsolvent, the pure water flux of membranes increases. At the same time, with an increase in the PN, the PVP rejection coefficient of membranes slightly decreases: from 93 to 85%. A more abrupt increase in the membrane flux is observed in a PN range of 39.7–125 g/dL. The maximum membrane flux and the lowest PVP rejection coefficient are observed for casting solutions containing a glycerol–PEG-400 nonsolvent with PN = 750 g/dL. An increase in the membrane flux with an increase in the PN of the nonsolvent is explained by differences in the supramolecular structure of polymer solutions, which affect the kinetics of phase separation and, accordingly, the structure and properties of the resulting membrane [46, 47].

Effect of the PN of the Nonsolvent on the Membrane Structure

Electron microscope studies of the membrane structure showed that, at a constant degree of saturation of the casting solution, the PN of the nonsolvent practically does not affect on the cross-sectional structure of membranes (Fig. 8). The structure of all the samples can be characterized as follows: a dense selective layer is followed by a less dense intermediate (or transition) layer, whose structure already contains structural elements (Figs. 8a–8d). The supporting

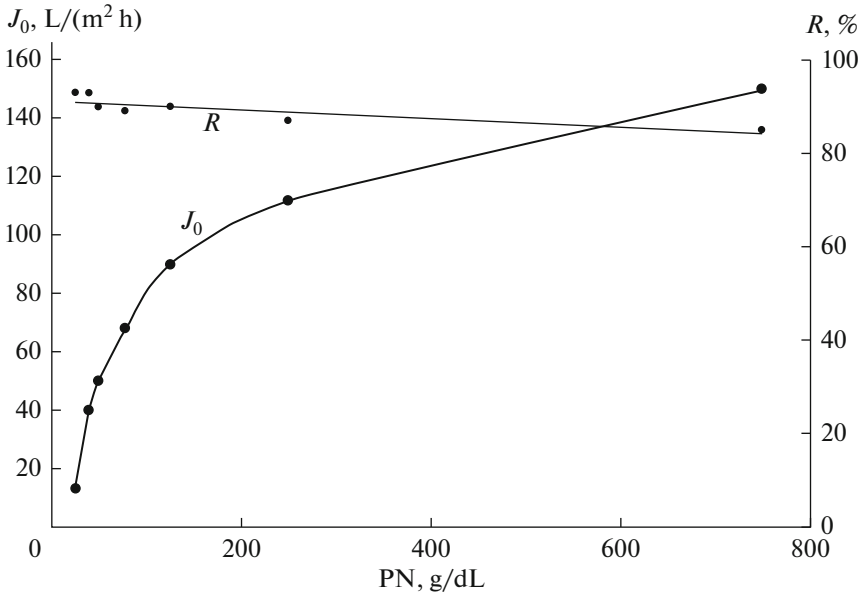

Fig. 7. Dependence of the pure water flux of membranes (J_0) and the PVP K-30 rejection coefficient (R) on the PN of the glycerol–PEG-400 nonsolvent.

layer of membranes does not have macrovoids; this fact is attributed to rather high degrees of saturation of the casting solutions ($\alpha^* = 0.94–0.95$). The only difference between the membrane structures is an increase in the selective layer thickness with an increase in the PN of the nonsolvent.

Determination of the thickness of the selective layer of membranes showed that, upon switching from PN = 39.7 g/dL to PN = 78.3 g/dL, the layer thickness increases from 1 to 2.5 μm; for PN = 750 g/dL, the selective layer thickness is 4.5 μm. In addition, with an increase in the PN, the porosity of the sublayer of membranes gradually decreases: a transfer from a fairly loose structure of the intermediate layer for PN = 39.7 g/dL (Fig. 8a) to a denser structure is observed. For PN = 750 g/dL (Fig. 8d), the structure of the matrix is the densest.

It is assumed that these structural changes can be associated with an increase in the viscosity of the casting solution [14] and differences in the selective layer structure, which is unresolvable by scanning electron microscopy (at a magnification of ×20000).

The surface topography of membranes was studied by atomic force microscopy. Figure 9 shows two- and three-dimensional atomic force microscopy images of PES membranes prepared from casting solutions containing a nonsolvent with various PNs. The light areas correspond to the highest points on the membrane surface, while the dark areas represent valleys. It was found that, with an increase in the PN of the nonsolvent in the casting solution, the area of valleys on the surface of the selective layer of membranes increases, while their shape changes from round to ellipsoidal. The PN of the nonsolvent also affects the surface roughness of the membrane. Table 2 provides information on the relationship between the PN of the nonsolvent in the casting solution and the root mean square surface roughness (R_q) and average roughness (R_a) at a scan area of 5 × 5 μm. With an increase in the PN from 39.7 to 750 g/dL, the R_a and R_q values increased from 6.4 to 41.9 and 8.2 to 58.0, respectively. The increase in R_a and R_q is attributed to an increase in the surface heterogeneity.

The results allow us to interpret the discrepancies in the scientific literature. Some of the authors claim that high-flux membrane structures are formed from casting solutions lying near the binodal, whereas other authors, conversely, believe that only low-flux membranes can be prepared from a casting solution lying near the bimodal. For example, Kim [43] suggested that membranes prepared from casting solutions with a higher nonsolvent-to-solvent weight ratio (PEG-600/NMP), i.e., from solutions with a higher degree of saturation, exhibit a higher flux. The results obtained by Kim can be attributed to the high PN value for PEG-600 (PN ≫ 1000 g/dL). In the case of membranes prepared from casting solutions containing a rather strong nonsolvent, low membrane flux values can be attributed to lower PN values. In this case, illustrative results were obtained by Sinha in [45], where the dependence of the membrane flux on the nonsolvent concentration in the casting solution exhibits an extreme behavior. The lowest membrane flux was recorded in the case of introduction of a maximum possible amount of the nonsolvent into the polymer solution. The existing discrepancy (concerning the high/low flux of membranes prepared from polymer–nonsolvent–solvent solutions and lying near the binodal line) is attributed to the difference in the PN of nonsolvents. The flux is low for strong nonsolvents and high for weak nonsolvents.

Table 2. Basic parameters of the surface roughness of membranes prepared from casting solutions containing nonsolvents of different hardness (with different PN values)

PN of nonsolvent, g/dL	R_a, nm	R_q, nm
37.9	6.4	8.2
50.4	10.2	13.2
78.3	34.5	42.5
750	41.9	58.0

The results make it possible to propose new approaches to preparing membranes with a desired structure and properties (flux). It was found that membranes with a spongy structure can be prepared only from casting solutions lying near the binodal line; the higher the PN of the nonsolvent contained in the casting solution, the higher the membrane flux. The highest membrane flux is recorded in the case of using casting solutions with a degree of saturation of $\alpha^* = 0.52–0.81$ (depending on the PN of the nonsolvent); in this case, macrovoids will be present in the structure of the supporting layer of membranes. The macrovoid size and shape also depend on the PN of the nonsolvent.

CONCLUSIONS

The effect of nonsolvent power on the structure and properties of ultrafiltration membranes prepared from PES–nonsolvent–DMAA casting solutions by the immersion precipitation method has been studied. Nonsolvent power has been characterized in terms of PN, i.e., the amount of the coagulant that leads to the phase separation of 100 mL of a 1% polymer solution. Nonsolvent power has been varied using mixtures of strong (glycerol, PN = 27.8 g/dL) and weak nonsolvents (PEG-400, PN > 1000 g/dL). It has been found that the use of a glycerol–PEG-400 mixture with various PN values as an additive to a PES solution makes it possible to control the region of existence of homogeneous solutions and their viscosity over a wide range. Membranes prepared from 22% PES solutions with a degree of saturation of $\alpha^* = 0.94–0.95$ are characterized by a pronounced spongy structure. It has

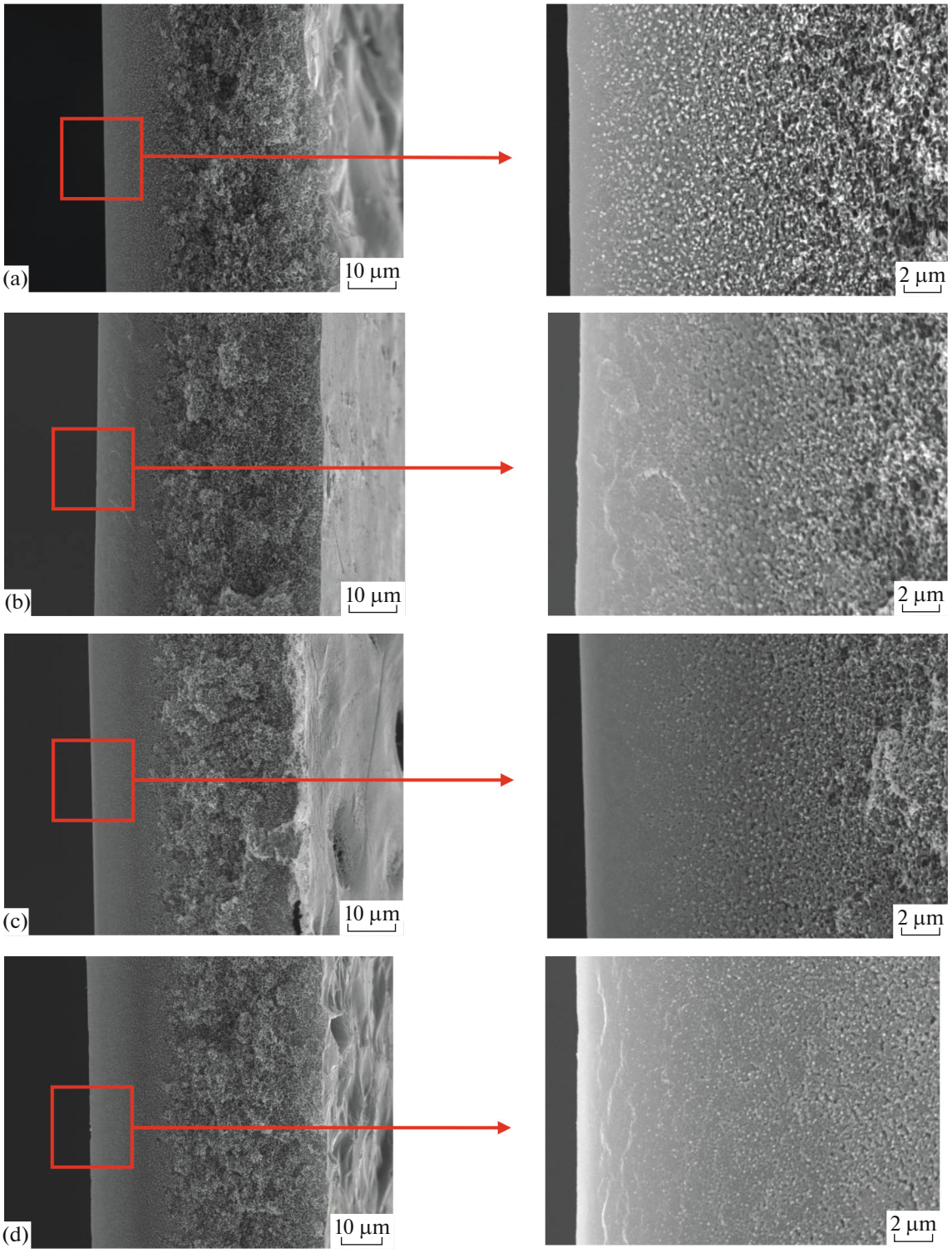

Fig. 8. Electron micrographs of cross section structure of PES membranes prepared from casting solutions with the addition of a mixed nonsolvent with the different PN values: (a) 39.7, (b) 78.3, (c) 125, and (d) 750 g/dL.

been found that an increase in the PN of the nonsolvent leads to an increase in the pure water flux of the membranes and a slight decrease in the rejection coefficient.

Using scanning electron microscopy, it has been found that an increase in the degree of saturation of casting solutions leads to a transition from an anisotropic membrane structure with a large number of mac-

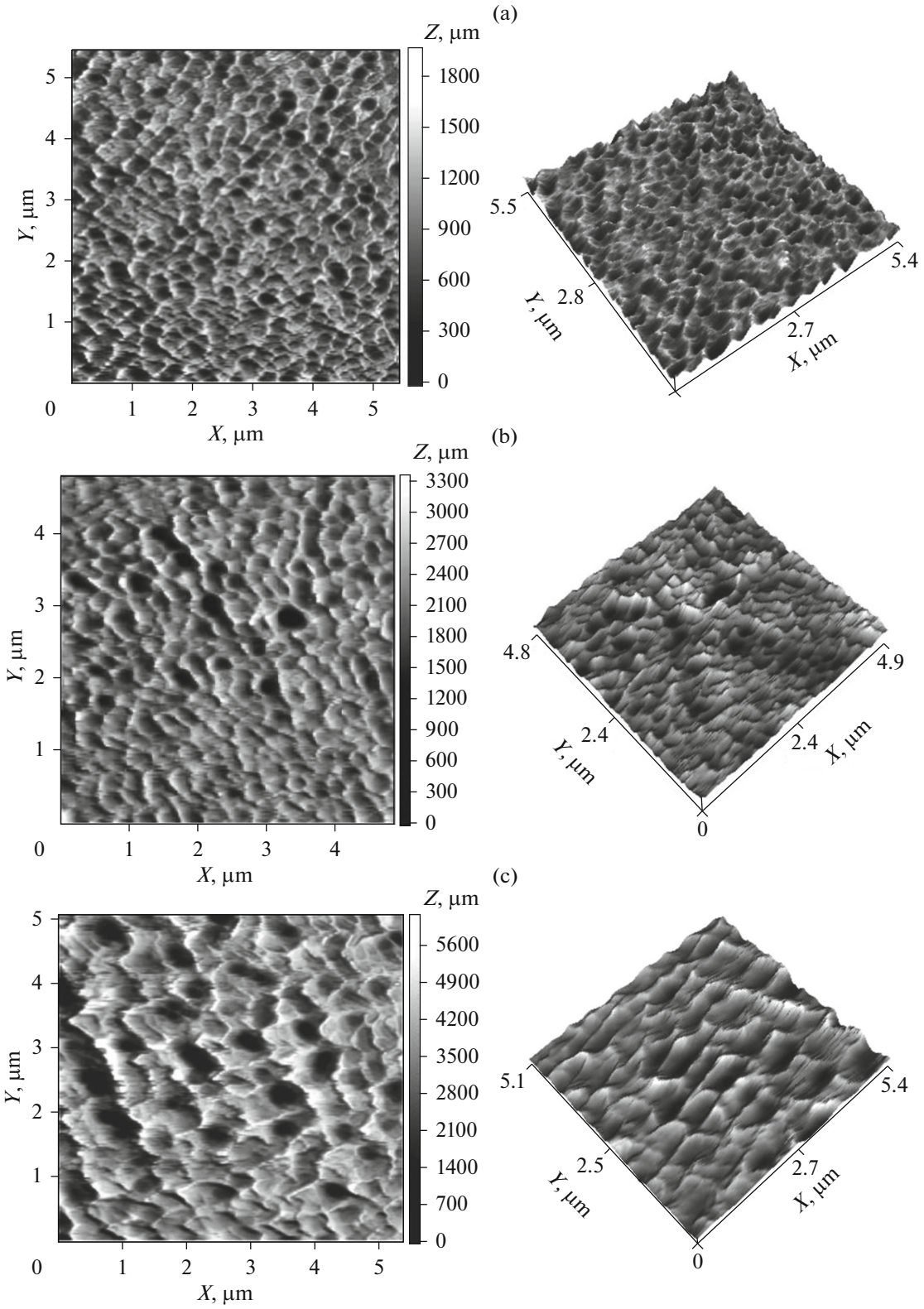

Fig. 9. Atomic force microscopy images of the selective surface of PES membranes prepared using nonsolvents with the following PNs: (a) 37.9, (b) 50.4, (c) 78.3, and (d) 750 g/dL.

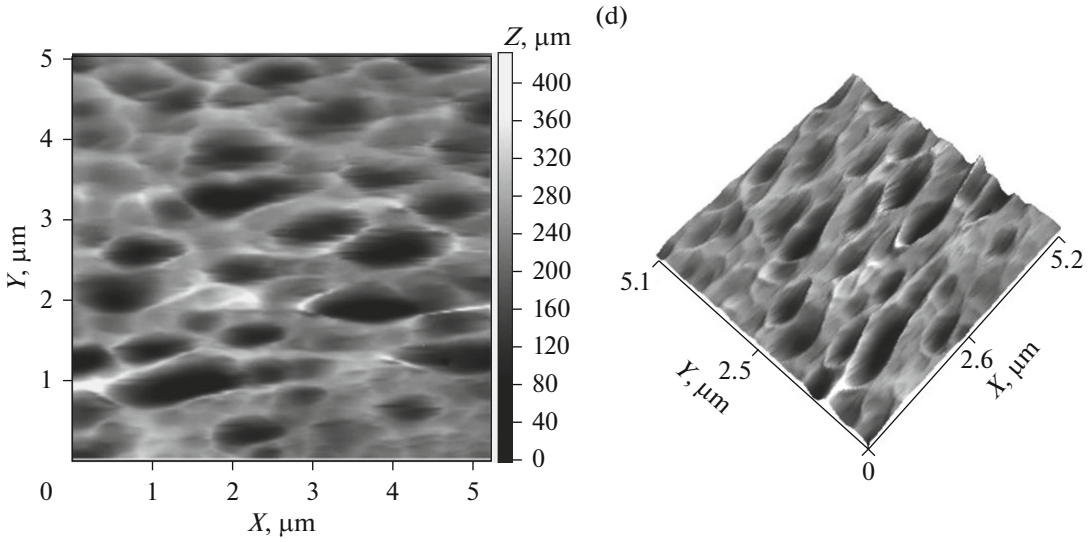

Fig. 9. (Contd.)

rovoids in the supporting layer to a spongy structure at $\alpha^* \geq 0.94$. Regardless of the power of the selected nonsolvent, the cross-sectional structure of membranes prepared from solutions with $\alpha = 0.94–0.95$ does not undergo significant changes; however, with an increase in the PN, an increase in the selective layer thickness is observed: upon switching from PN = 39.7 g/dL to PN = 750 g/dL, the layer thickness increases from 1 to 4.5 μm.

A new approach to obtaining membranes with a desired structure and properties has been proposed. Membranes with a spongy structure and a rather high flux (100–150 L/(m^2 h)) have been prepared from casting solutions located near the binodal line at a PN of the nonsolvent of ≥250 g/dL.

The highest flux ($J_0 \geq 200$ L/(m^2 h)) is recorded for membranes prepared from casting solutions with $\alpha^* = 0.52–0.81$. Large-sized macrovoids are dominant in the structure of these membranes.

FUNDING

This work was supported by the Belarusian Republican Foundation for Fundamental Research (project no. X18M-044).

REFERENCES

1. M. Mulder, *Basic Principles of Membrane Technology* (Kluwer, Dordrecht, 1991; Mir, Moscow, 1999).
2. C. A. Smolders, A. J. Reuvers, R. M. Boom, and I. M. Wienk, J. Membr. Sci. **73**, 259 (1992).
3. P. Witte, P. J. Dijkstra, J. W. A. Berg, and J. Feijen, J. Membr. Sci. **117**, 1 (1996).
4. D. Miller, D. Dreyer, C. Bielawski, D. Paul, and B. Freeman, Angew. Chem. **56**, 4662 (2017).
5. G. Arthanareeswaran and V. M. Starov, Desalination **267**, 57 (2011).
6. Y. Liu, G. H. Koops, and H. Strathmann, J. Membr. Sci. **223**, 187 (2003).
7. A. K. Holda and I. F. J. Vankelecom, J. Appl. Polym. Sci. **132**, 42130 (2015).
8. M. A. Aroona, A. F. Ismail, M. M. Montazer-Rahmati, and T. Matsuuraa, Sep. Purif. Technol. **72**, 194 (2009).
9. I.-Ch. Kim and K.-H. Lee, J. Membr. Sci. **230**, 183 (2004).
10. Z. Wang and J. Ma, Desalination **286**, 69 (2012).
11. P. S. T. Machado, A. C. Habert, and C. P. Borges, J. Membr. Sci. **155**, 171 (1999).
12. I. Wang, J. Ditter, R. Morris, and R. Kesting, US Patent No. 5959989 (1999).
13. A. Idris, M. J. Norashikin, and M. Y. Noordin, Desalination **207**, 324 (2007).
14. B. Chakrabarty, A. K. Ghoshal, and M. K. Purkait, J. Membr. Sci. **309**, 209 (2008).
15. I. Wang, J. Ditter, R. Morris, and R. Kesting, US Patent No. 5928774 (1999).
16. H. Pang, H. Gong, M. Du, Q. Shen, and Z. Chen, Sep. Purif. Technol. **191**, 38 (2018).
17. T. Wang, Ch. Zhao, P. Li, Y. Li, and J. Wang, Desalination **365**, 293 (2015).
18. J. Han, D. Yang, S. Zhang, and X. Jian, J. Membr. Sci. **345**, 257 (2009).
19. S.-J. Shin, J.-P. Kim, H.-J. Kim, J.-H. Jeon, and B.-R. Min, Desalination **186**, 1 (2005).
20. V. Laninovich, Desalination **186**, 39 (2005).
21. L. Zheng, Z. Wu, Y. Zhang, Y. Wei, and J. Wang, J. Eng. Sci. **45**, 28 (2016).
22. J. M. A. Tan, S.-H. Noh, G. Chowdhurry, and T. Matsuura, J. Membr. Sci. **174**, 225 (2000).
23. D. Wang, W. K. Teo, and K. Li, J. Membr. Sci. **204**, 247 (2002).

24. Y. Feng, G. Han, T.-S. Chung, M. Weber, N. Widjo, and C. Maletzk, J. Membr. Sci. **531**, 27(2017).
25. D. Wang, K. Li, and W. K. Teo, J. Membr. Sci. **176**, 147 (2000).
26. M. Sadrzadeh and S. Bhattacharjee, J. Membr. Sci. **441**, 31 (2013).
27. L. Wang, Z. Li, J. Ren, S.-G. Li, and C. Jiang, J. Membr. Sci. **275**, 46 (2006).
28. Z. Li and C. Jiang, J. Appl. Polym. Sci. **82**, 283 (2001).
29. J. Ren, Z. Li, and F.-S. Wong, J. Membr. Sci. **241**, 305 (2004).
30. B. Torrestiana-Sanchez, R. I. Ortiz-Basurto, La Brito-De, and E. Fuente, J. Membr. Sci. **152**, 19 (1999).
31. D. Wang, K. Li, and W. K. Teo, J. Membr. Sci. **115**, 85 (1996).
32. D. Wang, K. Li, and W. K. Teo, J. Membr. Sci. **98**, 233 (1995).
33. D. Wang, K. Li, S. Sourirajan, and W. K. Teo, J. Appl. Polym. Sci. **50**, 1693 (1993).
34. S. A. Pratsenko and A. V. Bil'dyukevich, Vysokomol. Soedin., Ser. A **36**, 457 (1994).
35. H. A. Tsai, M. J. Hong, G. S. Huang, Y. C. Wang, C. L. Li, K. R. Lee, J. and Y. Lai, J. Membr. Sci. **208**, 233 (2002).
36. A. V. Bil'dyukevich, S. A. Pratsenko, and T. V. Plisko, Khim. Tekhnol. **3**, 174 (2012).
37. J.-Y. Lai, F.-C. Lin, C.-C. Wang, and D.-M. Wang, J. Membr. Sci. **118**, 49 (1996).
38. L.-W. Chen and T.-H. Young, J. Membr. Sci. **59**, 15 (1991).
39. C. W. Yao, R. P. Burford, A. G. Fane, and C. J. D. Fell, J. Membr. Sci. **38**, 113 (1988).
40. K.-Y. Chun, S.-H. Jang, H.-S. Kim, Y.-W. Kim, and H.-S. Han, J. Membr. Sci. **169**, 197 (2000).
41. S. P. Papkov, *Physicochemical Fundamentals of Processing Polymer Solutions* (Khimiya, Moscow, 1971) [in Russian].
42. A. Zyabitskii, *Theoretical Foundations of Fiber Formation* (Khimiya, Moscow, 1979) [in Russian].
43. J.-H. Kim and K.-H. Lee, J. Membr. Sci. **138**, 153 (1998).
44. S. Darvishmanesh, C. Jansen, F. Taselli, E. Tocci, and B.-V. Bruggen, J. Membr. Sci. **379**, 60 (2011).
45. M. K. Sinha and M. K. Purkait, Desalination **338**, 106 (2014).
46. A. V. Bil'dyukevich, T. V. Plisko, Ya. A. Isaichikova, and A. A. Ovcharova, Membr. Membr. Tekhnol. **8**, 224 (2018).
47. A. A. Tager and O. G. Botvinnik, Vysokomol. Soedin., Ser. A **26**, 1284 (1974).

Translated by M. Timoshinina